

1981

# Critical exponents for the percolation problem and the Yang-Lee edge singularity

O. F. de Alcantara Bonfim  
*University of Portland*, bonfim@up.edu

J. E. Kirkham

A. J. McKane

Follow this and additional works at: [http://pilot scholars.up.edu/phy\\_facpubs](http://pilot scholars.up.edu/phy_facpubs)



Part of the [Physics Commons](#)

---

## Citation: Pilot Scholars Version (Modified MLA Style)

Bonfim, O. F. de Alcantara; Kirkham, J. E.; and McKane, A. J., "Critical exponents for the percolation problem and the Yang-Lee edge singularity" (1981). *Physics Faculty Publications and Presentations*. 4.  
[http://pilot scholars.up.edu/phy\\_facpubs/4](http://pilot scholars.up.edu/phy_facpubs/4)

This Journal Article is brought to you for free and open access by the Physics at Pilot Scholars. It has been accepted for inclusion in Physics Faculty Publications and Presentations by an authorized administrator of Pilot Scholars. For more information, please contact [library@up.edu](mailto:library@up.edu).

# Critical exponents for the percolation problem and the Yang–Lee edge singularity

O F de Alcantara Bonfim<sup>†</sup>, J E Kirkham<sup>‡</sup> and A J McKane<sup>§</sup>

<sup>†</sup> Department of Physics, University of Edinburgh, James Clerk Maxwell Building, Mayfield Road, Edinburgh EH9 3JZ, Scotland

<sup>‡</sup> Department of Theoretical Physics, University of Oxford, 1 Keble Road, Oxford OX1 3NP, England

<sup>§</sup> Department of Physics, University of Pennsylvania, Philadelphia, PA 19104, USA

Received 11 February 1981

**Abstract.** We give details of a calculation of critical exponents for a class of field theory models which have an interaction cubic in the fields. The results of the calculation, which we have already reported, give the exponents to third order in  $\varepsilon$  where  $\varepsilon = 6 - d$  and  $d$  is the dimensionality of space. The class of models includes the percolation problem and the Yang–Lee edge singularity and we give explicit results for the exponents to order  $\varepsilon^3$  in these cases. By using resummation methods, based on the asymptotic behaviour of the  $\varepsilon$  expansion, we obtain numerical estimates for these exponents for a number of interesting values of  $d$ .

## 1. Introduction

Within the last few years the renormalisation group approach to critical phenomena, as well as providing a qualitative understanding of the subject, has begun to give quantitative predictions for the critical exponents, whose accuracy is comparable to those obtained from high-temperature series. This has largely been due to the increased understanding of the structure of the perturbation series in field theory (Lipatov 1977, Brézin *et al* 1977) allowing more sophisticated resummation methods to be used to obtain more accurate critical exponents. Most of these calculations have been performed for the field theory with quartic interaction  $(\phi)^2$ ,  $\phi = (\phi_1, \phi_2, \dots, \phi_n)$ , both for the renormalisation group functions calculated directly in three dimensions (Baker *et al* 1978, Le Guillou and Zinn-Justin 1977, 1980) and through the  $\varepsilon$  expansion (Vladimirov *et al* 1979).

Recently, we reported the results of performing a three-loop calculation of critical exponents in models with an interaction which is cubic in the fields (de Alcantara Bonfim *et al* (1980), to be referred to as I). This gave critical exponents to order  $\varepsilon^3$  in  $6 - \varepsilon$  dimensions. In this paper we give details of the calculation and also, using resummation methods mentioned above, we obtain numerical values for the exponents from the  $\varepsilon$ -expansion results. We restrict ourselves to the exponents for the percolation problem and for the Yang–Lee edge singularity, since as explained in I we believe the  $\varepsilon$  expansion to be well defined in these cases, unlike some other models based on  $\phi^3$  theories.

The outline of the paper is as follows. In § 2 we discuss the renormalisation scheme we use, going into some detail concerning the method of evaluation of the Feynman diagrams. In § 3 the results of the calculation are presented and the critical exponents for the percolation problem and the Yang–Lee edge singularity are given explicitly to order  $\varepsilon^3$ . The resummation techniques used to resum the  $\varepsilon$  expansions are described in § 4 and the numerical estimates for exponents given in § 5. In § 6 we compare these estimates with those obtained using other methods. There are two appendices. In the first various integrals which appear in the calculation are evaluated and in the second we tabulate the values of the Feynman diagrams.

## 2. Renormalisation scheme

In this section we will describe the renormalisation scheme which was used to calculate the exponents for the general  $\phi^3$  Hamiltonian

$$H = \int d^d x \left[ \frac{1}{2}(\nabla\phi)^2 + \frac{1}{2}m^2\phi^2 + (g_0/3!)d_{ijk}\phi_i\phi_j\phi_k \right]. \quad (2.1)$$

In this case  $\phi$  is an  $n$ -component field,  $\phi^2 = \sum_{i=1}^n \phi_i\phi_i$ ,  $(\nabla\phi)^2 = \sum_{\mu=1}^d \sum_{i=1}^n (\nabla_{\mu}\phi_i)^2$  and  $d_{ijk}$  is an invariant third-rank tensor of some symmetry group. We choose to work in a general theory for two reasons. The first is to allow easy specialisation to different models. The second is that the tensor contractions of the  $d_{ijk}$  which arise are independent, hence for instance the 't Hooft identities ('t Hooft 1973) are satisfied for each tensor contraction separately. This enables us to classify the Feynman diagrams.

If we introduce a renormalised field  $\phi_{Ri} = \phi_i Z^{-1/2}$ , a renormalised coupling  $g_R$  and a renormalised mass  $m_R$ , we can write our Hamiltonian (2.1) as

$$H = \int d^d x \left[ \frac{1}{2}(\nabla\phi_R)^2 + \frac{1}{2}m_R^2\phi_R^2 + (g_R/3!)\mu^{\varepsilon/2} Z d_{ijk}\phi_{Ri}\phi_{Rj}\phi_{Rk} + \frac{1}{2}(\nabla\phi_R)^2(Z-1) \right. \\ \left. + \frac{1}{2}m_R^2(Z_2-1)\phi_R^2 + (1/3!)(u_0 Z^{3/2} - g_R)\mu^{\varepsilon/2} d_{ijk}\phi_{Ri}\phi_{Rj}\phi_{Rk} \right] \quad (2.2)$$

where  $u_0 = g_0\mu^{-\varepsilon/2}$  is the dimensionless coupling constant,  $\mu$  is a momentum scale,  $Z_2 = (m^2/m_R^2)Z$  is the mass renormalisation and we have included all counterterms explicitly. The role of the counterterms is to make the renormalised vertex functions finite and this allows us to calculate  $Z$ ,  $Z_2$  and  $g_R$ . The renormalisation group  $\beta$  function can now be found using

$$\beta(g_R) = -\frac{1}{2}\varepsilon(\partial \ln u_0 / \partial g_R)^{-1} \quad (2.3)$$

(Amit 1978) and hence the fixed point  $g^*$  from  $\beta(g^*) = 0$ . Critical exponents are then determined from the renormalisation group functions evaluated at the fixed point; for example, the exponent  $\eta$  is given by

$$\eta = \gamma_{\phi}(g^*)$$

where

$$\gamma_{\phi}(g_R) = \beta(g_R) \partial \ln Z / \partial g_R. \quad (2.4)$$

We use the minimal subtraction scheme of 't Hooft and Veltman (1972) to evaluate the vertex functions. This simplifies the calculation because we only have to evaluate divergent parts of the Feynman diagrams, i.e. pure multipoles in  $\varepsilon$ . The use of this

scheme introduces a further simplification since it allows any choice of the external momenta of the vertex. This was shown explicitly at the two-loop level by Amit (1976). We choose to evaluate the three-point function at zero external momentum in a massive theory. The renormalised three-point vertex function is

$$(\Gamma_R^{(3)})_{ijk} = g_R \mu^{\epsilon/2} d_{ijk} + A_1 d_{ijk} + \mu^{\epsilon/2} (u_0 Z^{3/2} - g_R) d_{ijk} + \dots \tag{2.5}$$

where  $A_1$  is the value of the graph shown in appendix 2, table A1(a). Each of the terms on the right-hand side of the above equation is proportional to  $d_{ijk}$ , so we can define

$$(\Gamma_R^{(3)})_{ijk} = \Gamma_R^{(3)} d_{ijk}.$$

$\Gamma_R^{(3)}$  is finite by construction, so the counterterm  $\mu^{\epsilon/2} [u_0 Z^{3/2} - g_R]$  must exactly cancel the  $\epsilon$  pole from the triangle diagram at lowest order, hence

$$u_0 Z^{3/2} - g_R = -g_R^3 \beta / \epsilon + O(g_R^5) \tag{2.6}$$

where  $d_{ijk} \beta = d_{ilm} d_{jln} d_{kmn}$ .

In order to simplify the calculation of the two- and three-loop contributions we use the skeleton technique (Vladimirov 1979). To see how this works, let us consider the evaluation of the graphs (appendix 2, table A1(b)) at two loops. The contribution of the proper two-loop graph is

$$3 g_R^5 \mu^{5\epsilon/2} \beta^2 \int_{p,k} \frac{1}{(k^2 + m_R^2)^3 (p^2 + m_R^2)^2 [(k+p)^2 + m_R^2]} \tag{2.7}$$

where  $\int_{p,k}$  denotes  $\int [d^d k / (2\pi)^d] \int [d^d p / (2\pi)^d]$ . We use the identity

$$\frac{1}{p^2 + m^2} = \frac{1}{p^2} - \frac{m^2}{p^2(p^2 + m^2)} \tag{2.8}$$

to expand the propagators in the  $p$ -subintegration and obtain the result

$$\int_{p,k} \frac{1}{(k^2 + m_R^2)^3 p^4 (k+p)^2} \left( 1 - \frac{2m_R^2}{p^2 + m_R^2} + \frac{m_R^4}{(p^2 + m_R^2)^2} \right) \left( 1 - \frac{m_R^2}{(k+p)^2 + m_R^2} \right). \tag{2.9}$$

The only divergent part is

$$\int_{p,k} \frac{1}{(k^2 + m_R^2)^3 p^4 (k+p)^2}$$

which can easily be evaluated using the Feynman parameter method (see for instance Amit (1978)). The counterterm graph equals

$$-g_R^5 \frac{3}{\epsilon} \mu^{3\epsilon/2} \beta^2 k_d \int_k \frac{1}{(k^2 + m_R^2)^3}. \tag{2.10}$$

The sum of the divergent parts of the two graphs is (appendix 2, table A1(b))

$$\frac{3}{\epsilon^2} k_d^2 \mu^{\epsilon/2} \beta^2 g_R^5 \left[ \frac{1}{2} \left( \frac{\mu}{m} \right)^{2\epsilon} \left( 1 - \frac{5\epsilon}{4} \right) - \left( \frac{\mu}{m} \right)^\epsilon \left( 1 - \frac{3\epsilon}{4} \right) \right] \tag{2.11}$$

where  $k_d = S_d / (2\pi)^d$  and  $S_d$  is the surface area of a unit sphere in  $d$  dimensions. If we expand  $(\mu/m)^\epsilon$  and  $(\mu/m)^{2\epsilon}$  we find that the divergent parts  $(1/\epsilon) \ln(\mu/m)$  cancel between the two terms. This is a consequence of the fact that the minimal subtraction scheme is independent of the choice of momentum scale. Since these are the only terms

proportional to  $\beta^2$  we notice that this cancellation is satisfied for each independent tensor contraction.

We also have a contribution at this order multiplying  $\alpha\beta$  where  $\delta_{ij}\alpha = d_{ilm}d_{jim}$  (appendix 2, table A1(c)). The two-loop graph equals

$$\frac{3}{2}g_R^5\mu^{5\epsilon/2}\alpha\beta \int_{p,k} \frac{1}{(k^2+m_R^2)^4[(k+p)^2+m_R^2](p^2+m_R^2)}. \tag{2.12}$$

If we expand the  $p$ -subintegration in the masses we obtain

$$\frac{3}{2}g_R^5\mu^{5\epsilon/2}\alpha\beta \int_{p,k} \frac{1}{(k^2+m_R^2)^4(k+p)^2p^2} \left( 1 - \frac{2m_R^2}{p^2+m_R^2} + \frac{m_R^4}{(p^2+m_R^2)[(p+k)^2+m_R^2]} \right). \tag{2.13}$$

Clearly the last term is convergent, the first term is  $O(1/\epsilon^2)$  and the middle term  $O(1/\epsilon)$ . The value of this term is

$$-g_R^5\mu^{5\epsilon/2}\frac{3}{\epsilon}k_d\alpha\beta \int_k \frac{k^{-\epsilon}}{(k^2+m_R^2)^4}m_R^2.$$

It is this term which we expect to be cancelled by the mass-counterterm graph which has the value

$$-3m_R^2(Z_2-1)\beta g_R^3\mu^{3\epsilon/2} \int_k \frac{1}{(k^2+m_R^2)^4}, \tag{2.14}$$

where  $(Z_2-1)$  can be found to be  $-g_R^2\alpha k_d/\epsilon$  from a one-loop calculation of  $\Gamma^{(2)}(q=0, m_R^2)$ . So we see that this exactly cancels the divergent part of the middle term in (2.13). To summarise the skeleton technique tells us that when the counterterms are included explicitly we may set all masses in the subintegrations to zero and ignore mass counterterms. We do not give a general proof for this theorem and we always check that it is satisfied explicitly for each set of diagrams.

We now illustrate how the skeleton technique works for a set of three-loop diagrams (appendix 2, table A1(e)). Consider the first diagram; it gives a contribution

$$3g_R^7\mu^{7\epsilon/2}\beta^3 \int_{s,p,k} \frac{1}{(k^2+m_R^2)^3(p^2+m_R^2)^2[(p-k)^2+m_R^2](s^2+m_R^2)^2[(s-p)^2+m_R^2]} \tag{2.15}$$

to  $\Gamma_R^{(3)}$ . If we expand the subintegrations in the masses using equation (2.8) and retain only the divergent parts, then we obtain

$$\begin{aligned} & 3g_R^7\mu^{7\epsilon/2}\beta^3 \int_{s,p,k} \frac{1}{(k^2+m_R^2)^3p^4(p-k)^2s^4(s-p)^2} \\ & \times \left( 1 - \frac{2m_R^2}{p^2+m_R^2} - \frac{m_R^2}{(p-k)^2+m_R^2} + \frac{m_R^4}{(p^2+m_R^2)^2} \right. \\ & \left. + \frac{2m_R^4}{(p^2+m_R^2)[(p-k)^2+m_R^2]} - \frac{m_R^6}{(p^2+m_R^2)^2[(p-k)^2+m_R^2]} \right). \end{aligned} \tag{2.16}$$

The first term has a  $(1/\epsilon^3)$  leading divergence and is the only one we expect to

contribute. The contribution of the counterterm (appendix 2, table A1(e)) is

$$\begin{aligned}
 & -g_R^7 \frac{1}{\epsilon} 3k_d \mu^{5\epsilon/2} \beta^3 \int_{p,k} \frac{1}{(k^2 + m_R^2)^3 p^4 (p-k)^2} \\
 & \times \left( 1 - \frac{2m_R^2}{p^2 + m_R^2} - \frac{m_R^2}{(p-k)^2 + m_R^2} + \frac{m_R^4}{(p^2 + m_R^2)^2} \right. \\
 & \left. + \frac{2m_R^4}{(p^2 + m_R^2)[(p-k)^2 + m_R^2]} - \frac{m_R^6}{(p^2 + m_R^2)^2[(p-k)^2 + m_R^2]} \right). \quad (2.17)
 \end{aligned}$$

The terms which are only  $1/\epsilon$  divergent from this counterterm exactly cancel those from the three-loop diagram. This shows explicitly the validity of the skeleton technique in this case. The resulting integrals can easily be evaluated using Feynman parameters. This is not always possible; for instance, the next graph in the same group gives rise to an integral

$$\int_{p,k} \frac{1}{p^2 k^4 (k-p)^2 (k-s)^2 (p-s)^2}$$

which has to be evaluated using more sophisticated techniques which we describe in appendix 1. In appendix 2 we give the results for the contributions to the three-point vertex function for each set of graphs which have the same skeleton structure. We have checked that the technique is valid to this order explicitly. We showed that within a set of graphs of the same skeleton structure the divergent contributions from  $(\mu/m)^{a\epsilon}$  factors cancel. This gives an immediate check on the leading behaviour of the diagrams. We now have

$$u_0 Z^{3/2} - g_R = a_1 g_R^3 + a_2 g_R^5 + a_3 g_R^7 + O(g_R^9) \quad (2.18)$$

where the  $a_i$  are all known.

The wavefunction renormalisation  $Z$  can be evaluated from

$$\Gamma^{(2)}(q^2, m_R^2) = q^2 + m_R^2 + (Z-1)q^2 + (Z_2-1)m_R^2 - \Sigma \quad (2.19)$$

where  $\Sigma$  is the sum of all connected one-particle-irreducible diagrams with two external legs. One method would be to consider  $m_R = 0$ , whence  $Z$  would be given in terms of the two-point diagrams at zero mass. However this is not the best scheme as some of the three-loop diagrams are very complicated. An alternative and better approach is to consider

$$\left. \frac{\partial}{\partial q^2} \{ \Gamma^{(2)}(q^2, m_R^2) \} \right|_{q^2=0} = 1 + (Z-1) - \left. \frac{\partial}{\partial q^2} \{ \Sigma \} \right|_{q^2=0}. \quad (2.20)$$

$Z$  is then given by derivatives of two-point functions, and the evaluation of these derivatives leads to integrals that are either identical to those from the three-point function or of order  $1/\epsilon^2$ . This means that there are only a few new integrals to evaluate. We consider the set of graphs (b) in appendix 2, table A2. The two-loop graph gives a contribution

$$\frac{\alpha\beta}{2} g_R^4 \mu^{2\epsilon} \int_{k,p} \frac{1}{(p^2 + m_R^2)(k^2 + m_R^2)[(p-k)^2 + m_R^2][(p-q)^2 + m_R^2][(k-q)^2 + m_R^2]}. \quad (2.21)$$

If we differentiate with respect to  $q^2$ , then set  $q^2 = 0$ , we obtain

$$\alpha\beta g_R^4 \mu^{2\epsilon} \int_{k,p} \frac{1}{(p^2 + m_R^2)^3 (k^2 + m_R^2)^2 [(p-k)^2 + m_R^2]} \left( -1 + \frac{4p^2}{d(p^2 + m_R^2)} + \frac{2k \cdot p}{d(k^2 + m_R^2)} \right) \tag{2.22}$$

since in this case

$$\lim_{q^2 \rightarrow 0} \left( \frac{q^\mu q^\nu}{q^2} \int_p \frac{p^\mu p^\nu}{p^2} f(p^2) + O(q) \right) = \frac{1}{d} \int_p f(p^2).$$

The total contribution for this graph and its counterterm is

$$\begin{aligned} & \left( \frac{4}{d} - 1 \right) \alpha\beta g_R^4 \left( \mu^{2\epsilon} \int_{k,p} \frac{1}{(p^2 + m_R^2)^3 (k^2 + m_R^2)^2 [(p-k)^2 + m_R^2]} - \frac{1}{\epsilon} \mu^\epsilon \int_p \frac{1}{(p^2 + m_R^2)^3} \right) \\ & - \frac{4}{d} \alpha\beta g_R^4 \left( \mu^{2\epsilon} \int_{k,p} \frac{m_R^2}{(p^2 + m_R^2)^4 (k^2 + m_R^2)^2 [(p-k)^2 + m_R^2]} \right. \\ & \left. - \frac{1}{\epsilon} \mu^\epsilon \int_p \frac{m_R^2}{(p^2 + m_R^2)^4} \right) \\ & + \frac{2}{d} \alpha\beta g_R^4 \mu^{2\epsilon} \int_{k,p} \frac{k \cdot p}{(p^2 + m_R^2)^3 (k^2 + m_R^2)^3 [(k-p)^2 + m_R^2]}. \end{aligned} \tag{2.23}$$

The first term contains exactly the same integrals as in the  $\beta^2$  graph (see equation (2.7)) and its counterterm (see equation (2.10)) in  $\Gamma_R^{(3)}$ . The second term is convergent, hence the third term is the only new integral to evaluate. This integral is straightforward as it is only  $O(1/\epsilon)$  divergent.

For the special case of total self-energy graphs ( $\alpha^2, \alpha^3$ ) this is not the best method. Instead, we evaluate the diagrams at zero mass and then differentiate with respect to  $q^2$ . Each diagram is then proportional to  $(\mu/q)^{a\epsilon}$  where  $a$  is the number of loops. The divergent contributions from these cancel, showing again that the results are independent of the choice of mass and momentum scale. The results for all the diagrams are given in appendix 2, table A2. We can now evaluate  $u_0$  in terms of  $g_R$  from equation (2.18), and so  $\beta(g_R)$ ,  $g^*$  and  $\eta$ . The results for these functions are given in § 3.

There remains one problem, the evaluation of  $Z_2$ . A possible method is to consider  $\Gamma^{(2)}(q^2 = 0, m_R^2)$  but this is very tedious and involves the reexpansion of the integrals using partial  $p$  (appendix 1). A more efficient method is to calculate  $\Gamma_R^{(2,1)}$ , the two-point vertex function with one  $\phi^2$  insertion. The renormalisation associated with  $\Gamma_R^{(2,1)}$  is the same as the mass renormalisation because we can write the massive vertex function as an expansion in the massless vertex functions with  $\phi^2$  insertions (Amit 1978).

$$\Gamma_R^{(2,1)} = 1 + C_1 + (Z_2 - 1) + \dots \tag{2.24}$$

where  $C_1$  is the value of the graph shown in figure 1. Hence we can calculate  $(Z_2 - 1)$  using minimal subtraction. The integrals are precisely those for the three-point vertex function; the multiplicities are different. The sets of diagrams to be summed are also the same, and we are able to use the results of table A1, appendix 2 directly. We do not draw the diagrams; there are two types, those which arise by adding an insertion to each line in every diagram in the two-point vertex and those which have a  $\Gamma^{(2,1)}$  counterterm vertex. There are 115 diagrams in all. We can then calculate

$$\nu^{-1} - 2 + \eta = \gamma_{\phi^2}(g^*)$$

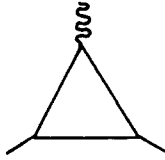


Figure 1. One-loop contribution to  $\Gamma^{(2,1)}$ .

where

$$\gamma_{\phi^2}(g_R) = \beta(g_R) \partial \ln Z_2 / \partial g_R. \tag{2.25}$$

The results are given in § 3.

### 3. Renormalisation functions and critical exponents

In this section we list the  $\varepsilon$ -expansion results for the renormalisation functions and the exponents for a general  $\phi^3$  theory. We then consider the calculation of the tensor contractions  $\alpha, \beta, \gamma, \delta, \lambda$  for the two cases of interest: the Yang–Lee edge singularity and the percolation problem. We give the exponents for these models explicitly.

Using the results for Feynman diagrams given in appendix 2 and the methods described in § 2, we can calculate the renormalisation constants

$$Z_1 - 1 \equiv \frac{u_0 Z^{3/2}}{g_R} - 1 = \sum_{\nu=1}^{\infty} \sum_{r=\nu}^{\infty} \frac{a_{\nu r} g_R^r}{\varepsilon^{\nu}}, \tag{3.1}$$

$$Z_2 - 1 = \sum_{\nu=1}^{\infty} \sum_{r=\nu}^{\infty} \frac{b_{\nu r} g_R^r}{\varepsilon^{\nu}}, \tag{3.2}$$

$$Z - 1 = \sum_{\nu=1}^{\infty} \sum_{r=\nu}^{\infty} \frac{c_{\nu r} g_R^r}{\varepsilon^{\nu}}, \tag{3.3}$$

to order  $g_R^6$  (the renormalisation constants are even in  $g_R$ ) within the minimal subtraction scheme ('t Hooft 1973). The pole coefficients  $a_{\nu r}, b_{\nu r}$  and  $c_{\nu r}$  are functions of the tensor contraction coefficients  $\alpha, \beta, \gamma, \delta, \lambda$ . They are not all independent; since the theory is renormalisable they will satisfy the 't Hooft identities ('t Hooft 1973). These can be derived most easily by calculating  $\beta(g_R), \gamma_{\phi}(g_R)$  and  $\gamma_{\phi^2}(g_R)$  from equations (3.1)–(3.3) for a general  $a_{\nu r}, b_{\nu r}$  and  $c_{\nu r}$ , and then demanding that they are finite as  $\varepsilon \rightarrow 0$ , i.e. that the coefficients of  $1/\varepsilon$  and  $1/\varepsilon^2$  vanish. This gives

$$\beta(g_R) = -\frac{1}{2}\varepsilon g_R + (a_{12} - \frac{3}{2}c_{12})g_R^3 + 2(a_{14} - \frac{3}{2}c_{14})g_R^5 + 3(a_{16} - \frac{3}{2}c_{16})g_R^7 + O(g_R^9), \tag{3.4}$$

$$\gamma_{\phi}(g_R) = -c_{12}g_R^2 - 2c_{14}g_R^4 - 3c_{16}g_R^6 + O(g_R^8), \tag{3.5}$$

$$\gamma_{\phi^2}(g_R) = -b_{12}g_R^2 - 2b_{14}g_R^4 - 3b_{16}g_R^6 + O(g_R^8), \tag{3.6}$$

with nine 't Hooft identities, of which we give only the three simplest for illustrative purposes:

$$\begin{aligned} c_{24} + c_{12}^2 - c_{12}a_{12} &= 0, \\ 2a_{24} - 3c_{24} - 3(c_{12} - a_{12})^2 &= 0, \\ 2b_{24} - b_{12}^2 - 2a_{12}b_{12} + 3b_{12}c_{12} &= 0. \end{aligned} \tag{3.7}$$



Our calculation of the renormalisation constants yields the following results for the pole coefficients:

$$a_{12} = -\beta, \quad b_{12} = -\alpha, \quad c_{12} = -\frac{1}{6}\alpha, \quad (3.8)$$

$$a_{24} = (\frac{3}{2}\beta^2 - \frac{1}{4}\alpha\beta), \quad b_{24} = (\frac{1}{4}\alpha^2 + \alpha\beta), \quad c_{24} = (\frac{1}{6}\alpha\beta - \frac{1}{36}\alpha^2),$$

$$a_{14} = (-\frac{3}{8}\beta^2 + \frac{7}{48}\alpha\beta - \frac{1}{4}\gamma), \quad b_{14} = (\frac{1}{48}\alpha^2 - \frac{1}{2}\alpha\beta), \quad c_{14} = (\frac{11}{432}\alpha^2 - \frac{1}{18}\alpha\beta), \quad (3.9)$$

$$a_{36} = (-\frac{5}{2}\beta^3 + \frac{11}{12}\alpha\beta^2 - \frac{1}{12}\alpha^2\beta), \quad b_{36} = (-\frac{1}{3}\alpha^2\beta - \frac{4}{3}\alpha\beta^2),$$

$$c_{36} = (-\frac{5}{648}\alpha^3 + \frac{1}{12}\alpha^2\beta - \frac{2}{9}\alpha\beta^2), \quad a_{26} = (\frac{43}{432}\alpha^2\beta - \frac{37}{48}\alpha\beta^2 + \frac{11}{8}\beta^3 - \frac{1}{12}\alpha\gamma + \frac{11}{12}\beta\gamma),$$

$$b_{26} = (\frac{1}{27}\alpha^3 + \frac{7}{6}\alpha\beta^2 + \frac{1}{3}\alpha\gamma), \quad c_{26} = (\frac{11}{864}\alpha^3 - \frac{61}{648}\alpha^2\beta + \frac{17}{108}\alpha\beta^2 + \frac{1}{18}\alpha\gamma),$$

$$a_{16} = [\frac{3}{16}\beta^3 + \frac{11}{72}\alpha\beta^2 - \frac{119}{2592}\alpha^2\beta + \beta\gamma(\frac{5}{6}\zeta(3) - \frac{71}{72}) + \frac{11}{144}\alpha\gamma - \frac{1}{3}\delta + \lambda(\frac{1}{3} - \zeta(3))], \quad (3.10)$$

$$b_{16} = [-\frac{95}{648}\alpha^3 + \alpha^2\beta(\frac{79}{288} + \frac{1}{6}\zeta(3)) + \alpha\beta^2(-\frac{65}{144} - \frac{1}{3}\zeta(3)) - \frac{7}{24}\alpha\gamma],$$

$$c_{16} = [-\frac{821}{93312}\alpha^3 + \frac{179}{5184}\alpha^2\beta - \frac{85}{2592}\alpha\beta^2 + \alpha\gamma(\frac{1}{36}\zeta(3) - \frac{7}{144})],$$

where  $\zeta(3) = \sum_{n=1}^{\infty} 1/n^3 = 1.202 \dots$  and where as usual a factor of  $k_d$  has been absorbed into  $g_R^2$ . The tensor contractions  $\alpha, \beta, \gamma, \delta, \lambda$  are defined in I, and discussed further later in this section.

We have checked that the nine 't Hooft identities are satisfied by these pole coefficients (the reader can easily check this for the three simple identities (3.7)). This is an important check on our calculation, especially since the identities must hold for all  $\alpha, \beta, \gamma, \delta, \lambda$ . Substitution of equations (3.8)–(3.10) into equations (3.4)–(3.6) gives the renormalisation group functions reported in I. The two-loop results agree with those appearing in the literature, in the cases where the same renormalisation scheme was used (Macfarlane and Woo 1974, Amit 1976).

The fixed point  $g^{*2}$ , given by  $\beta(g^*) = 0$ , and the critical exponents were given in I; we list them again for completeness:

$$g^{*2} = \frac{2\varepsilon}{(\alpha - 4\beta)} + \frac{\varepsilon^2}{(\alpha - 4\beta)^3} (\frac{11}{9}\alpha^2 - \frac{22}{3}\alpha\beta + 12\beta^2 + 8\gamma)$$

$$+ \frac{\varepsilon^3}{(\alpha - 4\beta)^5} [\frac{49}{216}\alpha^4 - \frac{1127}{324}\alpha^3\beta + \frac{1415}{54}\alpha^2\beta^2 - \frac{1048}{9}\alpha\beta^3 + 216\beta^4$$

$$+ \alpha^2\gamma(\frac{47}{9} + 4\zeta(3)) + \beta^2\gamma(-\frac{560}{3} + 320\zeta(3)) + \alpha\beta\gamma(\frac{104}{3} - 96\zeta(3))$$

$$+ 32\delta(\alpha - 4\beta) + 32\lambda(\alpha - 4\beta)(3\zeta(3) - 1) + 64\gamma^2] + O(\varepsilon^4), \quad (3.11)$$

$$\eta = \frac{\alpha\varepsilon}{3(\alpha - 4\beta)} + \frac{\alpha\varepsilon^2}{(\alpha - 4\beta)^3} [\frac{1}{27}\alpha\beta + \frac{2}{9}\beta^2 + \frac{4}{3}\gamma]$$

$$+ \frac{\alpha\varepsilon^3}{(\alpha - 4\beta)^5} [-\frac{7}{108}\alpha^3\beta + \frac{637}{486}\alpha^2\beta^2 - \frac{292}{27}\alpha\beta^3 + \frac{736}{27}\beta^4 + \frac{11}{27}\alpha^2\gamma$$

$$+ \alpha\beta\gamma(\frac{176}{27} - \frac{32}{3}\zeta(3)) + \beta^2\gamma(-\frac{80}{3} + \frac{128}{3}\zeta(3)) + \frac{32}{3}\gamma^2$$

$$+ \frac{16}{3}\delta(\alpha - 4\beta) + \frac{16}{3}\lambda(\alpha - 4\beta)(3\zeta(3) - 1)] + O(\varepsilon^4), \quad (3.12)$$

$$\begin{aligned} \nu^{-1} - 2 + \eta = & \frac{2\alpha\epsilon}{(\alpha - 4\beta)} + \frac{\alpha\epsilon^2}{(\alpha - 4\beta)^3} \left( \frac{19}{18}\alpha^2 - \frac{8}{3}\alpha\beta - 4\beta^2 + 8\gamma \right) \\ & + \frac{\alpha\epsilon^3}{(\alpha - 4\beta)^5} \left[ \frac{85}{24}\alpha^4 - \alpha^3\beta \left( \frac{2534}{81} + 4\zeta(3) \right) + \alpha^2\beta^2 \left( \frac{812}{9} + 40\zeta(3) \right) \right. \\ & - \alpha\beta^3 \left( \frac{1216}{9} + 128\zeta(3) \right) + \beta^4 \left( \frac{592}{3} + 128\zeta(3) \right) + \alpha^2\gamma \left( \frac{98}{9} + 4\zeta(3) \right) \\ & + \alpha\beta\gamma(16 - 96\zeta(3)) + \beta^2\gamma(320\zeta(3) - \frac{608}{3}) \\ & \left. + 64\gamma^2 + 32\delta(\alpha - 4\beta) + 32\lambda(\alpha - 4\beta)(3\zeta(3) - 1) \right] + O(\epsilon^4). \end{aligned} \tag{3.13}$$

These agree with the  $O(\epsilon^2)$  results of Priest and Lubensky (1976) and Amit† (1976), and with the  $O(\epsilon^3)$  evaluation of  $\eta$  in the special case of a symmetry for which  $\beta = \gamma = \lambda = 0$  (McKane 1977).

The simplest case of interest is the one where  $n = 1$  and  $g$  is purely imaginary, this being the model considered by Fisher (1978) in his study of Yang-Lee edge singularities. This effectively means  $d_{111} = i$ , leading to  $\alpha = \beta = \delta = \lambda = -1$  and  $\gamma = 1$ . Substituting these values into equation (3.12) gives

$$\eta = -\frac{\epsilon}{9} - \frac{43\epsilon^2}{3^6} + \epsilon^3 \left( -\frac{8375}{2^2 3^{10}} + \frac{16\zeta(3)}{3^5} \right) + O(\epsilon^4). \tag{3.14}$$

The exponent  $\sigma$  which characterises the Yang-Lee edge singularity is related to  $\eta$  by

$$\sigma = (d - 2 + \eta) / (d + 2 - \eta). \tag{3.15}$$

Field theoretic arguments show, as indicated in I, that the critical exponents  $\eta$  and  $\nu$  are not independent but related through the expression  $\nu^{-1} = \frac{1}{2}(d - 2 + \eta)$ . Therefore we shall not be interested in the exponent  $\nu$  in this case.

The other special case of interest is the percolation problem, which is given by the  $n \rightarrow 0$  limit of the  $(n + 1)$ -state Potts model (Fortuin and Kasteleyn 1972). The tensor  $d_{ijk}$  for the Potts model may be conveniently expressed in terms of the set of  $n + 1$  vectors  $e^\alpha$  which define the  $(n + 1)$  vertices of a hypertetrahedron in  $n$  dimensions (Zia and Wallace 1975):

$$d_{ijk} = \sum_{\alpha} e_i^\alpha e_j^\alpha e_k^\alpha \tag{3.16}$$

where the  $e_i^\alpha$  satisfy

$$\sum_{\alpha=1}^{n+1} e_i^\alpha = 0, \quad \sum_{\alpha=1}^{n+1} e_i^\alpha e_j^\alpha = (n + 1)\delta_{ij}, \quad \sum_{i=1}^n e_i^\alpha e_i^\beta = (n + 1)\delta^{\alpha\beta} - 1. \tag{3.17}$$

The contractions  $\alpha, \beta, \gamma, \delta, \lambda$  can be calculated using equation (3.17). For example, the coefficient  $\alpha$  is defined by

$$\alpha\delta_{ij} = d_{ilm}d_{jlm} \tag{3.18}$$

which is equal to

$$\sum_{\alpha,\beta} e_i^\alpha e_j^\beta [(n + 1)\delta_{\alpha\beta} - 1][(n + 1)\delta_{\alpha\beta} - 1] = (n + 1)^2(n - 1)\delta_{ij} \tag{3.19}$$

and thus  $\alpha = (n + 1)^2(n - 1)$ . In this case it is easy to calculate the coefficient directly.

† There is a misprint in equation (6.23) of Amit's paper; the coefficient of  $\alpha_1\beta_1$  should be  $-\frac{1}{3}$  not  $+\frac{1}{3}$ .

However, the calculation of  $\lambda$  and  $\delta$  involves the contraction of seven tensors and it becomes convenient to use a diagrammatic technique to keep track of all the factors.

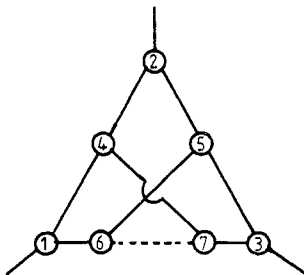
To illustrate this idea consider the evaluation of  $\lambda$  :

$$\lambda d_{ijk} = d_{i_1 i_2} d_{j_1 j_2} d_{k_1 k_2} d_{l_1 l_2} d_{m_1 m_2} d_{n_1 n_2} d_{o_1 o_2} \tag{3.20}$$

If we substitute for the  $d$ 's from equation (3.16) and then contract out the  $e$ 's using equation (3.17), we obtain

$$\begin{aligned} \lambda d_{ijk} = \sum_{\{\alpha\}} e_i^{\alpha_1} e_j^{\alpha_2} e_k^{\alpha_3} & [(n+1)\delta^{\alpha_1 \alpha_4} - 1] [(n+1)\delta^{\alpha_1 \alpha_6} - 1] [(n+1)\delta^{\alpha_2 \alpha_4} - 1] \\ & \times [(n+1)\delta^{\alpha_2 \alpha_5} - 1] [(n+1)\delta^{\alpha_3 \alpha_5} - 1] [(n+1)\delta^{\alpha_3 \alpha_7} - 1] \\ & \times [(n+1)\delta^{\alpha_4 \alpha_7} - 1] [(n+1)\delta^{\alpha_5 \alpha_6} - 1] [(n+1)\delta^{\alpha_6 \alpha_7} - 1]. \end{aligned} \tag{3.21}$$

If we multiply out the square brackets in equation (3.21) we obtain the product of nine  $\delta$ 's plus all products of eight  $\delta$ 's multiplied by  $(-1)$ , etc, until we get down to  $(-1)^9$  (up to factors of  $(n+1)$ ). Each product can be represented by a diagram such as shown in figure 2. The full lines correspond to the  $\delta$ 's and the broken lines to the  $(-1)$  factors. It is easy to convince oneself that if all three vertices are not connected to each other, then the diagram gives zero contribution to equation (3.21) by virtue of the result  $\sum_{\alpha} e^{\alpha} = 0$ . Thus we are able to evaluate (3.21) by counting up the number of 'connected' diagrams. In addition, if there are any 'clusters' of full lines within the connected diagram which are not connected to the vertices, there will be a free sum over the 'cluster', giving rise to an extra factor of  $(n+1)$ . This picture is very close to the physical ideas of percolation theory, and has been used by Houghton *et al* (1978) to reformulate the field theoretic model of percolation so as to avoid the  $n \rightarrow 0$  limit.



**Figure 2.** Diagrammatic representation of the tensor contraction  $\lambda$ .

Using these methods, we obtain the following results for the  $(n+1)$ -state Potts model:

$$\begin{aligned} \alpha &= (n+1)^2(n-1), \\ \beta &= (n+1)^2(n-2), \\ \gamma &= (n+1)^6 - 6(n+1)^5 + 10(n+1)^4, \\ \delta &= (n+1)^9 - 9(n+1)^8 + 29(n+1)^7 - 32(n+1)^6, \\ \lambda &= (n+1)^9 - 9(n+1)^8 + 29(n+1)^7 - 33(n+1)^6. \end{aligned} \tag{3.22}$$

When we take the  $n \rightarrow 0$  limit we obtain  $\alpha = -1, \beta = -2, \gamma = 5, \delta = -11$  and  $\lambda = -12$  for

the percolation problem. The substitution of these values into equations (3.12) and (3.13) gives

$$\eta = -\frac{\varepsilon}{21} - \frac{206\varepsilon^2}{3^3 7^3} + \left( -\frac{93619}{2 \times 3^5 7^5} + \frac{256\zeta(3)}{3 \times 7^4} \right) \varepsilon^3 + O(\varepsilon^4), \quad (3.23)$$

$$\nu^{-1} - 2 + \eta = -\frac{2\varepsilon}{7} - \frac{335\varepsilon^2}{2 \times 3^2 7^3} + \left( -\frac{235495}{2^3 3^4 7^5} + \frac{204\zeta(3)}{7^4} \right) \varepsilon^3 + O(\varepsilon^4). \quad (3.24)$$

We discuss the interpretation of these results, as well as those for the Yang–Lee singularity, in the next section.

#### 4. Resummation of the $\varepsilon$ expansion

The perturbation expansion in the coupling constant  $g$  for field theories has been shown to be asymptotic (Dyson 1952, Lipatov 1977). The  $\varepsilon$ -expansion series are also asymptotic; in particular, it can be shown that at high order the coefficient of  $\varepsilon^K$  has the form

$$K! a^K K^b c [1 + O(1/K)] \quad (4.1)$$

(Lipatov 1977, Brézin *et al* 1977). The values of  $a$  and  $b$  have been determined for some of the renormalisation functions in Houghton *et al* (1978) and Kirkham and Wallace (1979) for the percolation problem and Yang–Lee edge singularity respectively. We have extended these calculations to find  $a$  and  $b$  for the particular functions we wish to study. Our results for exponents are

$$\begin{aligned} \eta = \gamma_\phi(g^*) \quad \text{and} \quad \nu^{-1} - 2 + \eta = \gamma_{\phi^2}(g^*) \\ \text{have } b = \frac{9}{2} \quad \text{and} \quad a = \begin{cases} -\frac{5}{18} & \text{Yang–Lee edge,} \\ -\frac{15}{28} & \text{percolation.} \end{cases} \end{aligned} \quad (4.2)$$

In the remainder of this section, we show how the results obtained from high-order estimates can be incorporated into a resummation procedure of the  $\varepsilon$  expansion to give reasonable estimates for the critical exponents. In effect, these resummation procedures provide an analytic continuation of the  $\varepsilon$ -expansion series.

The simplest resummation method used was Padé approximants (Baker 1970), in which the series is replaced by a ratio of a polynomial of degree  $N$  to one of degree  $D$ . We shall refer to this as the  $[N, D]$  approximant.

In order to include the high-order behaviour of the  $\varepsilon$  expansion, more sophisticated resummation techniques are necessary. Let us write the  $\varepsilon$  expansion of the critical exponents in the form

$$f(\varepsilon) = \sum_K f_K (-\varepsilon)^K \quad (4.3)$$

where  $f_K$  behaves for large  $K$  as in (4.1). The function  $f(\varepsilon)$  is assumed to be analytic everywhere in the complex plane, except for a branch cut along the negative real axis. A convergent expansion may be obtained from (4.3) via its Borel transform,  $B(x)$  defined by

$$B(x) = \sum_K B_K (-x)^K \quad (4.4a)$$

where

$$B_K = f_K/a^K \Gamma(K + b + 1). \tag{4.4b}$$

In this way,  $B(x)$  is convergent inside the unit circle of the complex  $x$ -plane with the nearest singularity localised at  $x = -1$ . Using the integral representation of the  $\Gamma$  function,

$$\Gamma(K + b + 1) = \int_0^\infty e^{-t} t^{K+b} dt,$$

we can write (4.3) as

$$f(\varepsilon) = \frac{1}{a\varepsilon} \int_0^\infty dx \exp\left(-\frac{x}{a\varepsilon}\right) \left(\frac{x}{a\varepsilon}\right)^b B(x). \tag{4.5}$$

However, the series we have for  $B(x)$  is divergent along parts of the real axis, and so we cannot perform the integral in (4.5) until we have made an analytic continuation to the whole real axis. One method is to use a Padé approximant for  $B(x)$ . This gives the Padé Borel method.

An alternative way of analytically continuing the function  $B(x)$  in (4.5) is by means of an appropriate conformal mapping, which maps the whole positive, real axis into the region of convergence of the series for  $B(x)$ . A most convenient conformal transformation is that defined by

$$w = \frac{(1+x)^{1/2} - 1}{(1+x)^{1/2} + 1} \Leftrightarrow x = \frac{4w}{(1-w)^2} \tag{4.6}$$

which maps the whole complex  $x$ -plane into the interior of the unit circle of the  $w$  plane. The interval  $(0, \infty)$  of  $x$  is mapped into the interval  $(0, 1)$  of  $w$ , and the branch cut is mapped into the boundary of the unit circle,  $|w| = 1$ . The Taylor expansion for the function  $B[x(w)]$  is now convergent inside the unit circle  $|w| < 1$ . Writing (4.5) in terms of the new variable  $w$ , we obtain

$$f(\varepsilon) = \frac{4}{\varepsilon a} \int_0^1 dw \frac{(1+w)}{(1-w)^3} \left(\frac{4w}{\varepsilon a(1-w)^2}\right)^b \exp\left(-\frac{4w}{\varepsilon a(1-w)^2}\right) B[x(w)]. \tag{4.7}$$

The coefficient of  $w^p$  in the expansion of  $B[x(w)]$  can be written in terms of the  $f_K$ 's of the original expansion with  $K \leq p$ . A great improvement in this resummation method can be achieved, as proposed by Vladimirov *et al* (1979), if we include in (4.7) the information about the asymptotic behaviour of  $f(\varepsilon)$  for large  $\varepsilon$ , namely

$$f(\varepsilon) \underset{\varepsilon \rightarrow \infty}{\sim} \varepsilon^\lambda. \tag{4.8}$$

We rewrite  $B[x(w)]$  as

$$B[x(w)] = \left(\frac{x}{w}\right)^\lambda \sum_{K=1}^N B_K^{(\lambda)} w^K \tag{4.9}$$

in order to match the required asymptotic condition for  $f(\varepsilon)$ .

In soluble models, such as the anharmonic oscillator or a  $\phi^4$  field theory with a Gaussian propagator, where the asymptotic behaviour for large values of the coupling constant, namely

$$f(g) \underset{g \rightarrow \infty}{\sim} g^\lambda, \tag{4.10}$$

is known exactly, numerical experiments performed by Kazakov *et al* (1979) show that the best convergence for the approximants,  $f^N(g)$ , is obtained when the value of  $\lambda$  corresponds to the correct asymptotic value. Since the asymptotic values for large  $\varepsilon$  in the series for the critical exponents are not known, we shall identify the value of  $\lambda$  in (4.8) as the value which gives the expression

$$|\Delta_N| = |1 - f^N(\varepsilon)/f^{N-1}(\varepsilon)| \quad (4.11)$$

a sharp minimum. Here,  $f^N(\varepsilon)$  is the value of (4.7) when the first  $N$  terms of the initial  $\varepsilon$ -expansion are known. This method has been applied to a  $\phi^4$ -field theory with  $N = 4$  (Vladimirov *et al* 1979). The estimate for the critical exponents obtained from this method are in good agreement with experimental results and high-temperature series analysis. The value of  $\lambda$  has also been numerically estimated by another method (Tarasov 1979). This latter method consists of evaluating the asymptotic behaviour of  $f(\varepsilon)$  for large  $\varepsilon$ , from numerically estimated asymptotic forms of the coefficients,  $B_k^{(\lambda)}$ , in the limit  $k \rightarrow \infty$ . The value of  $\lambda$  estimated by both methods are in good agreement.

We shall now apply the resummation techniques described above to calculate the critical exponents for the Yang–Lee edge singularity and percolation problems. The various results obtained are subsequently compared with calculations performed using different theoretical techniques.

## 5. Numerical results

In § 3 we calculated the  $\varepsilon$  expansions for the critical exponents for the Yang–Lee edge singularity and percolation problem. In this section we report the results of applying the resummation methods of § 4 to these series.

In table 1 we show the results obtained for  $\eta$  for the Yang–Lee edge singularity from Padé [2, 1], Padé Borel [2, 1], and the conformal mapping techniques. We obtained the value of  $\lambda = 1.2$  from minimising  $\Delta$  as explained in § 4. In this table we note the recent estimates given by Kurtze and Fisher (1979) for the critical exponent  $\sigma$  using high-temperature series analyses. At  $d = 6$  we have the exact mean field theory and in  $d = 1$  the exact value of the linear chain Ising Model (Yang and Lee 1952).

In table 2 we list our results for exponents for the percolation problem. We applied the resummation schemes to  $\eta$  and  $\nu^{-1} - 2 + \eta$  and found  $\lambda = 1.2$  and 1.1 respectively in the conformal method. The  $\nu$  and  $\gamma$  given in the table were calculated from the resummed values of  $\eta$  and  $\nu^{-1} - 2 + \eta$  using scaling relations. We also list some results from other methods. A more complete list of other results can be found in Essam (1980) and Stauffer (1979).

## 6. Summary and discussion

Resummation techniques have been used to treat the  $\varepsilon$ -expansion series for the critical exponents obtained from the field-theoretic renormalisation group approach. Supplementary information from the high-order behaviour of the  $\varepsilon$ -expansion series and from its asymptotic form for large  $\varepsilon$  has been incorporated in an attempt to improve the estimates for the critical exponents. In figure 3, we indicate the functional dependence of the critical exponent,  $\sigma$ , on the dimensionality for the Yang–Lee edge singularity. We also show the exact results for lower and higher dimensionalities and

**Table 1.** Yang-Lee edge singularity.

Dimension	$\eta$	$\sigma$	$\sigma$
6	0	0.5	0.5 <sup>(a)</sup>
5	-0.145	0.400 <sup>(p)</sup>	
	-0.147	0.399 <sup>(pb)</sup>	
	-0.149	0.399 <sup>(cm)</sup>	
4	-0.317	0.266 <sup>(p)</sup>	
	-0.328	0.264 <sup>(pb)</sup>	
	-0.342	0.262 <sup>(cm)</sup>	
3	-0.498	0.091 <sup>(p)</sup>	
	-0.524	0.086 <sup>(pb)</sup>	0.086 ± 0.015 <sup>(b)</sup>
	-0.560	0.079 <sup>(cm)</sup>	
2	-0.683	-0.146 <sup>(p)</sup>	
	-0.728	-0.154 <sup>(pb)</sup>	-0.163 ± 0.003 <sup>(b)</sup>
	-0.797	-0.166 <sup>(cm)</sup>	
1	-0.869	-0.483 <sup>(p)</sup>	
	-0.938	-0.491 <sup>(pb)</sup>	-0.5 <sup>(a)</sup>
	-1.050	-0.506 <sup>(cm)</sup>	

<sup>(p)</sup> denotes results obtained using the [2, 1] Padé approximant.

<sup>(pb)</sup> denotes results obtained using the [2, 1] Padé Borel method.

<sup>(cm)</sup> denotes results obtained using the conformal mapping technique.

<sup>(a)</sup> are the exact results for six and one dimensions.

<sup>(b)</sup> are the estimates of Kurtze and Fisher (1979).

**Table 2.** Percolation problem.

Dimension	$\gamma = \nu(2 - \eta)$	$\gamma$	$\nu$	$\nu$
6	1	1	0.5	0.5
5	1.18 <sup>(p)</sup>	1.17 ± 0.02 <sup>(a)</sup>	0.57 <sup>(p)</sup>	
	1.18 <sup>(pb)</sup>	1.18 ± 0.07 <sup>(b)</sup>	0.57 <sup>(pb)</sup>	0.6 ± 0.1 <sup>(g)</sup>
	1.18 <sup>(cm)</sup>		0.57 <sup>(cm)</sup>	
4	1.43 <sup>(p)</sup>	1.40 ± 0.02 <sup>(a)</sup>	0.67 <sup>(p)</sup>	
	1.44 <sup>(pb)</sup>	1.48 ± 0.08 <sup>(b)</sup>	0.68 <sup>(pb)</sup>	0.7 ± 0.1 <sup>(g)</sup>
	1.45 <sup>(cm)</sup>		0.68 <sup>(cm)</sup>	
3	1.78 <sup>(p)</sup>	1.66 ± 0.07 <sup>(c)</sup>	0.82 <sup>(p)</sup>	
	1.81 <sup>(pb)</sup>	1.6 ± 0.1 <sup>(d)</sup>	0.83 <sup>(pb)</sup>	0.84 ± 0.01 <sup>(g)</sup>
	1.86 <sup>(cm)</sup>		0.84 <sup>(cm)</sup>	
2	2.33 <sup>(p)</sup>	2.43 ± 0.03 <sup>(e)</sup>	1.04 <sup>(p)</sup>	
	2.41 <sup>(pb)</sup>	2.42 ± 0.02 <sup>(a)</sup>	1.07 <sup>(pb)</sup>	1.35 ± 0.01 <sup>(g)</sup>
	2.54 <sup>(cm)</sup>	2.43 ± 0.03 <sup>(f)</sup>	1.11 <sup>(cm)</sup>	

<sup>(p)</sup> denotes results obtained using the [2, 1] Padé approximant.

<sup>(pb)</sup> denotes results obtained using the [2, 1] Padé Borel method.

<sup>(cm)</sup> denotes results obtained using the conformal mapping technique.

<sup>(a)</sup> are results of Fisch and Harris (1978).

<sup>(b)</sup> are results of Gaunt and Ruskin (1978).

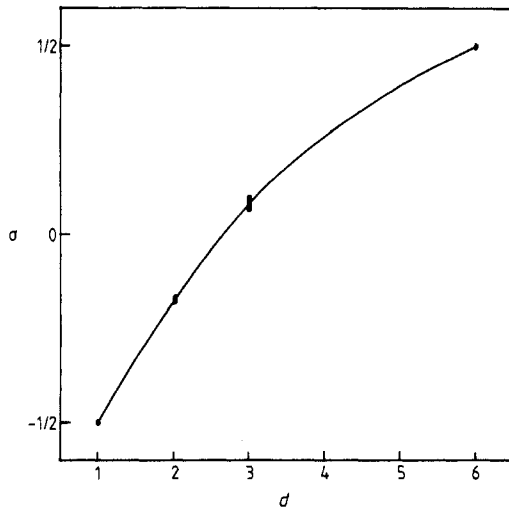
<sup>(c)</sup> are results of Sykes *et al* (1976a).

<sup>(d)</sup> are results of Sur *et al* (1977).

<sup>(e)</sup> are results of Sykes *et al* (1976b).

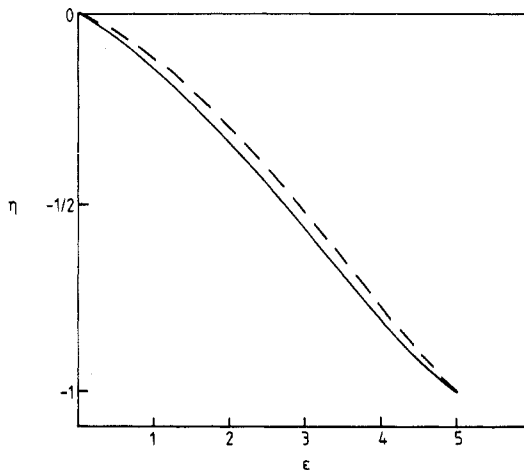
<sup>(f)</sup> are results of Nakanishi and Stanley (1978).

<sup>(g)</sup> are results of Stauffer (1979).



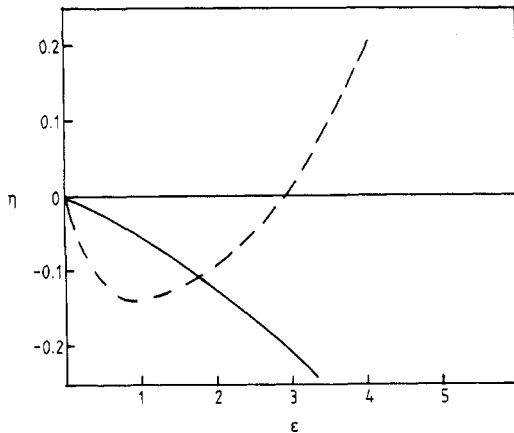
**Figure 3.** The dependence of the critical exponent  $\sigma$  on dimensionality. Points at one and six dimensions are exact. The full line is the resummed value obtained from the  $\varepsilon$  expansion. The solid bars are the high-temperature series estimates of Kurtze and Fisher (1979).

the high-temperature series estimates. As one can see, the agreement is very impressive, even for one dimension where one has to set  $\varepsilon = 5$ . In the case of the percolation problem, however, the results are not so good. From table 2, one sees that the agreement is quite reasonable down to and including four dimensions. For dimensions below four, the results for  $\gamma$ , for example, look unrealistic. However, this discrepancy can be better understood if one looks at the dependence of the critical exponent,  $\eta$ , upon the dimensionality  $d$ , as indicated schematically in figure 5. The complex structure of this critical exponent, in stark contrast to the structure of the same exponent



**Figure 4.** The dependence of the critical exponent  $\eta$  on dimensionality for the Yang-Lee edge singularity. The full line is the resummed value from the  $\varepsilon$  expansion. The broken line is the expected behaviour based on the estimates of Kurtze and Fisher (1979) and exact results at integer dimensionalities.





**Figure 5.** The dependence of the critical exponent  $\eta$  on dimensionality for the percolation problem. The full line is the resummed value from the  $\varepsilon$  expansion. The broken line indicates the shape of the expected behaviour based on estimates at integer dimensionalities taken from Stauffer (1979). The depth of the well is uncertain because the estimates for four and five dimensions are not scale invariant and we calculate  $\eta$  using scaling relations.

for the Yang–Lee edge singularity problem (see figure 4) seems to be the root of this disagreement. It is natural to expect that such behaviour in the dimensionality will not be reflected in a series with few terms. Finally, we conclude that although the estimates for the critical exponents are expected to be poorer as  $\varepsilon$  increases, the main source of discrepancy for the critical exponents of the percolation problem is the complex structure of the critical exponent  $\eta$ , and the inability of a series which has few terms to reproduce this structure.

**Acknowledgments**

We wish to thank Professor D J Wallace for communicating the work of the Dubna group to us and also for encouraging us to undertake the present calculation. In particular OFAB thanks Professor D J Wallace for invaluable help and CNPq (Brazilian Agency) for financial support. AJM wishes to thank the Department of Applied Mathematics and Theoretical Physics, University of Cambridge, where part of this work was carried out.

**Appendix 1. Evaluation of integrals**

In this appendix we will begin by explaining how the integrals which do not break down into repeated integrals of the type  $\int_p 1/p^{2\alpha}(p-q)^{2\beta}$  can be related to one another. We then discuss three possible methods of evaluation. The relevant integrals are

$$I_1 \equiv \int_{k,p} \frac{1}{k^2 p^2 (k-1)^2 (p-1)^2 (k-p)^2} \equiv k_d^2 \left( \frac{A_1}{\varepsilon^2} + \frac{B_1}{\varepsilon} + C_1 \right) + O(\varepsilon),$$

$$I_2 \equiv \int_{k,p} \frac{1}{k^4 p^2 (k-1)^2 (p-1)^2 (k-p)^2} \equiv k_d^2 \left( \frac{A_2}{\varepsilon^2} + \frac{B_2}{\varepsilon} + C_2 \right) + O(\varepsilon),$$

$$\begin{aligned}
 I_3 &\equiv \int_{k,p} \frac{1}{k^2 p^2 (k-1)^2 (p-1)^2 (k-p)^4} \equiv k_d^2 \left( \frac{B_3}{\varepsilon} + C_3 \right) + O(\varepsilon), \\
 I_4 &\equiv \int_{k,p} \frac{1}{k^4 p^2 (k-1)^4 (p-1)^2 (k-p)^2} \equiv k_d^2 \left( \frac{B_4}{\varepsilon} + C_4 \right) + O(\varepsilon), \\
 I_5 &\equiv \int_{k,p} \frac{1}{k^4 p^4 (k-1)^2 (p-1)^2 (k-p)^2} \equiv k_d^2 C_5 + O(\varepsilon), \\
 I_6 &\equiv \int_{k,p} \frac{1}{k^4 p^2 (k-1)^2 (p-1)^4 (k-p)^2} \equiv k_d^2 C_6 + O(\varepsilon), \\
 I_7 &\equiv \int_{k,p} \frac{1}{k^2 p^2 (k-1)^2 (p-1)^4 (k-p)^4} \equiv k_d^2 C_7 + O(\varepsilon),
 \end{aligned}
 \tag{A1.1}$$

where 1 represents a unit vector. We relate the integrals using the partial  $p$  method ('t Hooft and Veltman 1972). In this method we introduce a factor  $1 = (1/d) \sum_{\mu=1}^d \partial p_{\mu} / \partial p_{\mu}$  into our integral and integrate by parts. In particular, for the integral  $I = \int f(p) d^d p$

$$-dI = \int p_{\mu} \frac{\partial f(p)}{\partial p_{\mu}} d^d p
 \tag{A1.2}$$

provided that the surface terms vanish. For two integration variables we have

$$-2dI = \int_{p,k} p_{\mu} \frac{\partial f(p, k)}{\partial p_{\mu}} + \int_{p,k} k_{\mu} \frac{\partial f(p, k)}{\partial k_{\mu}}.
 \tag{A1.3}$$

The application of this to the first integral gives

$$(8-2d)I_1 = -2 \int_{p,k} \frac{1}{p^2 (k-1)^4 (p-1)^2 (k-p)^2} + 2 \int_{p,k} \frac{1}{k^2 p^2 (k-1)^4 (p-1)^2 (k-p)^2}.
 \tag{A1.4}$$

We notice that the second integral is  $I_2$  and the first integral can be evaluated using the Feynman parameter method. We therefore have the following equation between  $I_1$  and  $I_2$ :

$$(2\varepsilon - 4)I_1 = (1/3\varepsilon^2)[1 + \frac{7}{4}\varepsilon + \frac{25}{8}\varepsilon^2 + O(\varepsilon^3)] + 2I_2.
 \tag{A1.5}$$

If we apply the partial  $p$  method to the second integral we obtain

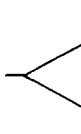

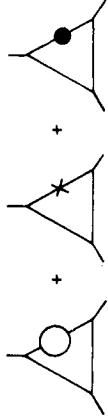

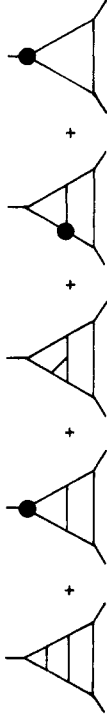

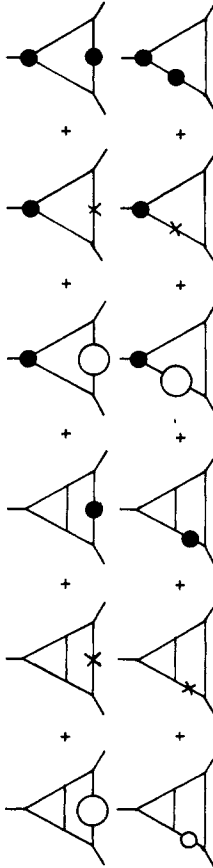


$$(2\varepsilon - 1)I_2 = I_4 + I_6 - (1/2\varepsilon^2)[1 + \frac{3}{4}\varepsilon + \frac{11}{8}\varepsilon^2 + O(\varepsilon^3)]
 \tag{A1.6}$$

and from the third integral

$$(\varepsilon - 1)I_3 = -(1/2\varepsilon)[1 + \frac{3}{4}\varepsilon + O(\varepsilon^2)] + I_7.
 \tag{A1.7}$$

We see from these relations that we can determine all the  $I_1 \dots I_7$  from  $I_5, I_6, I_7$  and one of  $I_1, I_2$  and  $I_4$ .  $I_5, I_6$  and  $I_7$  are all finite integrals and so we can calculate their leading behaviour by using Gegenbauer polynomials in momentum space (Nickel 1974). In

**Table A1.** Values of three-point diagrams.

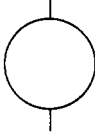
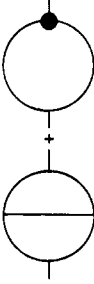
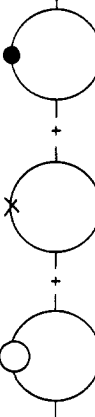
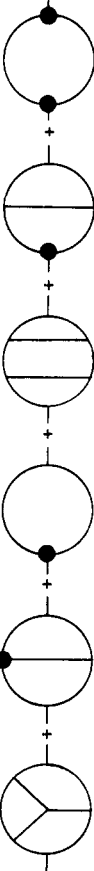
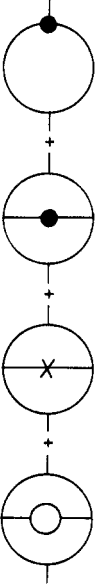
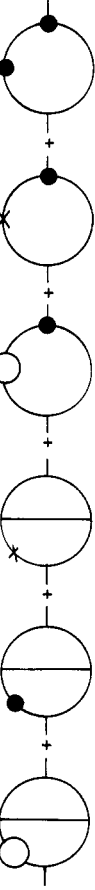
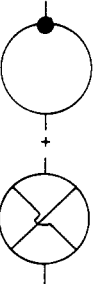
(a)		$= \frac{\beta}{\epsilon},$
(b)		$= -\frac{3\beta^2}{2\epsilon^2} \left(1 - \frac{\epsilon}{4}\right),$
(c)		$= \frac{\alpha\beta}{4\epsilon^2} \left(1 - \frac{7\epsilon}{12}\right),$
(d)		$= \frac{\gamma}{4\epsilon},$
(e)		$= \frac{3\beta^3}{2\epsilon^3} \left(1 - \frac{3\epsilon}{4} + \frac{\epsilon^2}{12}\right),$
(f)		$= \frac{\beta^3}{\epsilon^3} \left(1 - \frac{\epsilon}{4} + \frac{5\epsilon^2}{16}\right),$
(g)		$= -\frac{\beta^2\alpha}{6\epsilon^3} \left(1 - \frac{5\epsilon}{12} - \frac{47\epsilon^2}{144}\right),$
(h)		$= -\frac{\beta^2\alpha}{3\epsilon^3} \left(1 - \frac{5\epsilon}{12} - \frac{47\epsilon^2}{144}\right),$
(i)		$= -\frac{\beta^2\alpha}{6\epsilon^3} \left(1 - \frac{5\epsilon}{4} + \frac{23\epsilon^2}{48}\right),$

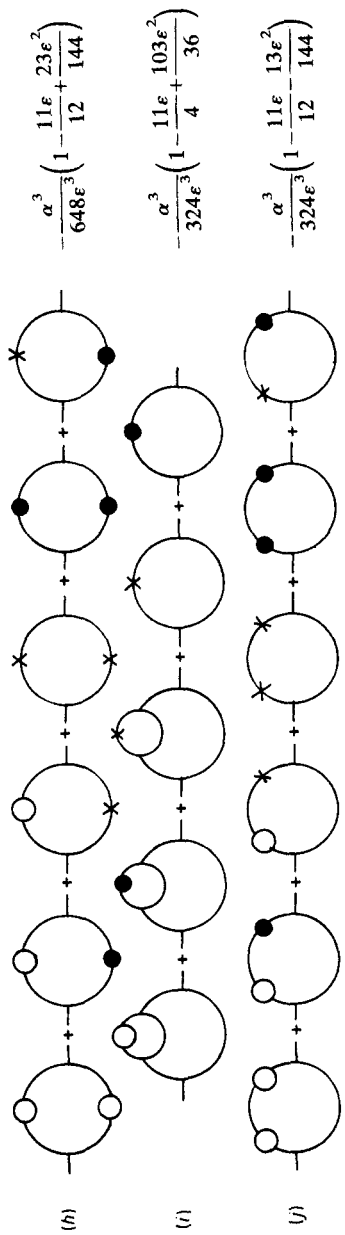
(j)									$= -\frac{\beta^2 \alpha}{4\epsilon^3} \left( 1 - \frac{17\epsilon}{12} + \frac{17\epsilon^2}{18} \right),$
(k)									$= \frac{\beta \alpha^2}{36\epsilon^3} \left( 1 - \frac{29\epsilon}{12} + \frac{19\epsilon^2}{9} \right),$
(l)									$= \frac{\beta \alpha^2}{36\epsilon^3} \left( 1 - \frac{7\epsilon}{12} - \frac{11\epsilon^2}{48} \right),$
(m)									$= \frac{\beta \alpha^2}{36\epsilon^3} \left( 1 - \frac{7\epsilon}{12} - \frac{11\epsilon^2}{48} \right),$
(n)									$= \frac{\alpha \gamma}{12\epsilon^2} \left( 1 - \frac{11\epsilon}{12} \right),$
(o)									$= -\frac{\beta \gamma}{4\epsilon^2} \left( 1 - \frac{\epsilon}{4} \right),$
(p)									$= -\frac{\beta \gamma}{6\epsilon^2} \left( 1 - \frac{23\epsilon}{12} + 2\epsilon \zeta(3) \right),$
(q)									$= -\frac{\beta \gamma}{2\epsilon} \left( 1 - \frac{29\epsilon}{24} + \epsilon \zeta(3) \right),$
(r)									$= \frac{\lambda}{\epsilon} \left( \zeta(3) - 3 \right).$

(s)

$$= \frac{\delta}{3\epsilon}$$

**Table A2.** Values of derivatives of two-point diagrams.

	Value of $\frac{d}{dP^2}$ (sum of graphs)
(a) 	$\frac{\alpha}{6\epsilon}$
(b) 	$\frac{\alpha\beta}{6\epsilon^2} \left(1 - \frac{\epsilon}{3}\right)$
(c) 	$-\frac{\alpha^2}{36\epsilon^2} \left(1 - \frac{11\epsilon}{12}\right)$
(d) 	$-\frac{2\alpha\beta^2}{9\epsilon^3} \left(1 - \frac{17\epsilon}{24} + \frac{85\epsilon^2}{576}\right)$
(e) 	
(f) 	$\frac{7\alpha^2\beta}{108\epsilon^3} \left(1 - \epsilon + \frac{295\epsilon^2}{1008}\right)$
(g) 	$\frac{\alpha\gamma}{18\epsilon^2} \left(1 + \frac{\epsilon\zeta(3)}{2} - \frac{7\epsilon}{8}\right)$



**Table A3.** Contributions to  $\Gamma_{\mathbb{R}}^{(2,1)}$ .

---


$$\begin{aligned}
 & (\alpha/\varepsilon)k_d g_{\mathbb{R}}^2 \\
 & -(\alpha\beta/\varepsilon^2)k_d^2 g_{\mathbb{R}}^4 (1 - \frac{1}{2}\varepsilon) \\
 & -(\alpha^2/4\varepsilon^2)k_d^2 g_{\mathbb{R}}^4 (1 + \frac{1}{2}\varepsilon) \\
 & (4\alpha\beta^2/3\varepsilon^3)k_d^3 g_{\mathbb{R}}^6 (1 - \frac{7}{8}\varepsilon + \frac{65}{192}\varepsilon^2 + \frac{1}{4}\zeta(3)\varepsilon^2) \\
 & (\alpha^2\beta/3\varepsilon^3)k_d^3 g_{\mathbb{R}}^6 (1 - \frac{79}{96}\varepsilon^2 - \frac{1}{2}\zeta(3)\varepsilon^2) \\
 & -(\alpha\gamma/3\varepsilon^2)k_d^3 g_{\mathbb{R}}^6 (1 - \frac{7}{8}\varepsilon) \\
 & -(\alpha^3/27\varepsilon^2)k_d^3 g_{\mathbb{R}}^6 (1 - \frac{95}{24}\varepsilon)
 \end{aligned}$$


---

particular, to evaluate only the leading term we can work in exactly six dimensions so that the polynomials are orthogonal. We also notice that  $I_6$  is equal to  $I_7$  at leading order; this is because they arise from the same irreducible graph (that associated with the tensor contraction  $\lambda$ ) as a result of different choices for the order of integration.

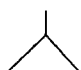
We also need to evaluate one of  $I_1, I_2$  or  $I_4$ . If we use Gegenbauer polynomials in momentum space for  $6 - \varepsilon$  dimensions, the polynomials are no longer exactly orthogonal and the only integral we can calculate to the required order in closed form is  $I_4$ . However this is sufficient. Another alternative is to make a Fourier transformation to real space where the Gegenbauer polynomials are exactly orthogonal (Chetyrkin *et al* 1980). This method allows all the integrals  $I_1, I_2, I_4$  to be calculated separately and also gives the results exactly in terms of  $\Gamma$  functions. This means that we can determine the integrals to any order in  $\varepsilon$ . The method is however more complex than the first. The third method is used to calculate  $I_1$  (although it could be used for the others) and involves the transformation of the integral into Minkowski space so that the diagram may be cut and the unitarity of the  $S$ -matrix exploited ('t Hooft and Veltman 1973, Drummond 1979). This method gives the result exactly in terms of  $\Gamma$  functions.

We list here the results for  $I_1 \dots I_7$  to the required accuracy:

$$\begin{aligned}
 I_1 &= -(k_d^2/3\varepsilon^2)[1 + \frac{3}{2}\varepsilon + \frac{35}{16}\varepsilon^2 + O(\varepsilon^3)], \\
 I_2 &= (k_d^2/2\varepsilon^2)[1 + \frac{3}{4}\varepsilon + \frac{7}{8}\varepsilon^2 + O(\varepsilon^3)], \\
 I_3 &= (k_d^2/2\varepsilon)[1 + (\frac{29}{12} - 2\zeta(3))\varepsilon + O(\varepsilon^2)], \\
 I_4 &= (k_d^2/\varepsilon)[1 + (\frac{4}{3} - \zeta(3))\varepsilon + O(\varepsilon^2)], \\
 I_5 &= k_d^2 + O(\varepsilon), \\
 I_6 &= (\zeta(3) - \frac{1}{3})k_d^2 + O(\varepsilon), \\
 I_7 &= I_6 + O(\varepsilon),
 \end{aligned}$$

where  $\zeta(3) = \sum_{n=1}^{\infty} n^{-3}$ .

**Appendix 2. Explanation of symbols used in tables**

 denotes the three-point vertex  $\frac{g_{\mathbb{R}}}{3!}d_{ijk}\mu^{\varepsilon/2}$ .

● denotes the counter term  $(1/3!)d_{ijk} [u_0 Z^{3/2} - g_{\mathbb{R}}]\mu^{\varepsilon/2}$ .

- denotes the propagator  $\frac{1}{p^2 + m_R^2}$ .
- $\times$ — denotes the counterterm  $\frac{(Z-1)p^2}{(p^2 + m_R^2)^2}$ .
- $\bullet$ — denotes the counterterm  $\frac{(Z_2-1)m_R^2}{(p^2 + m_R^2)^2}$ .

Each sum of three-point graphs is multiplied by  $(g_R)^a k_a^b \mu^{e/2}$  and each sum of two-point graphs is multiplied by  $(g_R)^a k_a^b$  where  $a$  = number of vertices,  $b$  = number of loops.

## References

- de Alcantara Bonfim O F, Kirkham J E and McKane A J 1980 *J. Phys. A: Math. Gen.* **13** L247
- Amit D J 1976 *J. Phys. A: Math. Gen.* **9** 1441
- 1978 *Field Theory, the Renormalization Group and Critical Phenomena* (New York: McGraw-Hill)
- Baker G A 1970 *The Padé Approximant in Theoretical Physics* ed. G A Baker and J L Gammel (New York: Academic)
- Baker G A, Nickel B G and Meiron D I 1978 *Phys. Rev. B* **17** 1365
- Brézin E, Le Guillou J C and Zinn-Justin J 1977 *Phys. Rev. D* **15** 1544
- Chetyrkin K G, Kataev A L and Tkachov F V 1980 *Nucl. Phys. B* **174** 345
- Drummond I T 1979 unpublished
- Dyson F J 1952 *Phys. Rev.* **85** 631
- Essam J W 1980 *Rep. Prog. Phys.* **43** 833
- Fisch R and Harris A B 1978 *Phys. Rev. B* **18** 416
- Fisher M E 1978 *Phys. Rev. Lett.* **40** 1610
- Fortuin C M and Kasteleyn P W 1972 *Physica* **57** 536
- Gaunt D S and Ruskin H 1978 *J. Phys. A: Math. Gen.* **11** 1369
- Le Guillou J C and Zinn-Justin J 1977 *Phys. Rev. Lett.* **39** 95
- 1980 *Phys. Rev. B* **21** 3976
- 't Hooft G 1973 *Nucl. Phys. B* **61** 455
- 't Hooft G and Veltman M 1972 *Nucl. Phys. B* **44** 189
- 1973 *Diagrammer CERN preprint*
- Houghton A, Reeve J S and Wallace D J 1978 *Phys. Rev. B* **17** 2956
- Kazakov D I, Tarasov O V and Shirkov D V 1979 *Tear. Mat. Fiz.* **38** 9
- Kirkham J E and Wallace D J 1979 *J. Phys. A: Math. Gen.* **12** L47
- Kurtze D A and Fisher M E 1979 *Phys. Rev. B* **20** 2785
- Lipatov L N 1977 *Sov. Phys.-JETP* **45** 216
- Macfarlane A J and Woo G 1974 *Nucl. Phys. B* **77** 91 and 1975 *Erratum B* **86** 548
- McKane A J 1977 *J. Phys. G: Nucl. Phys.* **3** 1165
- Nakanishi H and Stanley H E 1978 *J. Phys. A: Math. Gen.* **11** L189
- Nickel B G 1974 *Oxford preprint* (unpublished)
- Priest R G and Lubensky T C 1976 *Phys. Rev. B* **13** 4159 and 1976 *Erratum B* **14** 5125
- Stauffer D 1979 *Phys. Rep.* **54** 5125
- Sur A, Lebowitz J L, Marro J, Kalos M H and Kirkpatrick S 1977 *J. Statist. Phys.* **15** 345
- Sykes M F, Gaunt D S and Glen M 1976 *J. Phys. A: Math. Gen.* **9** 1705
- 1976 *J. Phys. A: Math. Gen.* **9** 97
- Tarasov O V 1979 *Lett. Math. Phys.* **3** 143
- Vladimirov A A 1979 *Tear. Mat. Fiz.* **36** 732
- Vladimirov A A, Kazakov D I and Tarasov O V 1979 *Sov. Phys.-JETP* **50** 521
- Yang C N and Lee T D 1952 *Phys. Rev.* **87** 404
- Zia R K P and Wallace D J 1975 *J. Phys. A: Math. Gen.* **8** 1495